RSC Advances

ROYAL SOCIETY OF CHEMISTRY

www.rsc.org/advances

Table of Contents

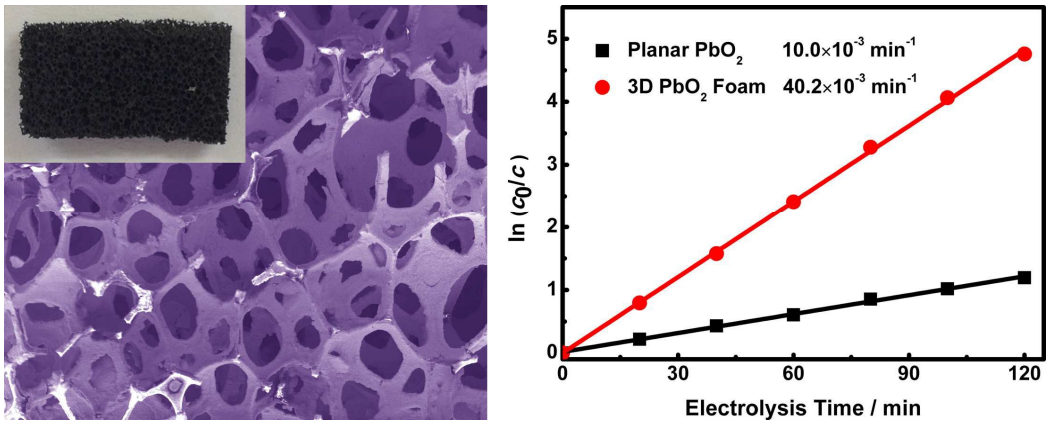

3D macroporous PbO_2 foam electrode possesses a binder-free and highly-through architecture, and ensures a high efficiency for degrading organic contaminants.

Novel three-dimensional macroporous PbO_2 foam electrode for efficient electrocatalytic decolorization of dyes

Tigang Duan, Ye Chen*, Qing Wen*, Yupeng Cong, Ying Duan, Yuyang Wang

Key Laboratory of Superlight Materials and Surface Technology of Ministry of Education, College of Materials Science and Chemical Engineering, Harbin Engineering University, Harbin, 15001, Heilongjiang, China

*Corresponding author.

Tel.: +86-13059004260.

Email-address: chenye511@126.com (Y Chen), wenqing@hrbeu.edu.cn (Q Wen).

Abstract

The electrode construction is the key factor for the efficient electrocatalytic degradation of organic contaminants. However, it is still a challenge to construct electrode architecture with large diffusion coefficient and high efficiency. Here, we used a facile method to successfully fabricate the three-dimensional macroporous foam architecture of PbO_2 electrode that possesses the same framework as the kitchen low-cost macroporous sponges. This 3D architecture is monolithic and possesses continuously through macroporores with high interconnection. Compared with the traditional planar PbO_2 electrode, 3D macroporous PbO_2 foam has greater electrochemical roughness (184 versus 4.05), significantly lowered electrochemical impedance (29.2 versus 410 ohm), and greater diffusion coefficient (41.8×10^{-6} versus

2.29×10^{-6} cm^2 s^{-1}). Moreover, the electrocatalytic dye decolorization experiments show that 3D macroporous PbO_2 foam possesses much larger first-order kinetics constant (40.2×10^{-3} versus 10.0×10^{-3} min^{-1} for highly concentrated orange II). Higher specific surface area, significantly enhanced mass transport, and excellent electrocatalytic activity of as-fabricated PbO_2 foam can make it as a promising electrocatalytic electrode for the wastewater treatment.

Key words: PbO_2 foam; macroporous; monolithic; enhanced mass transport

Introduction

With the rapid development of industry, varieties of toxic organic substances, such as phenolic compounds, azo free/azo dyes and other biologically refractory organic pollutants, have been widely used and have been quite hazardous to the environment and humans[1-3]. Conventional physical-chemical processes and biological treatments have not always been achieving satisfactory results; therefore, disposing organic pollutants efficiently has become an urgent problem[4-6]. In recent years, electrocatalytic oxidation technology, as one of advanced oxidation technologies, has been an attractive alternative for removing bio-refractory organic pollutants because of its easy operation, high efficiency, fast degradation rate and environmental friendliness[7-9]. It has been known that the effectiveness of electrocatalytic oxidation process largely depends on the properties of electrode materials[10]. Among all kinds of

metal oxide electrodes, PbO_2 anode has been widely used in electrocatalytic oxidation technology due to its low cost, long lifetime, and good stability[11-12]. To further enhance its performance, many researchers have made a great deal of research on the electrode modification. Thereinto, CNT modified electrodes have been proved to have excellent performance. For example, Duan et al. reported that the doping of CNT could effectively enhance the electrochemical activity and service time of PbO_2 electrode[13-14]. Ghasemi et al. also confirmed this result[15].

Up to date, two-dimensional electrodes have been most extensively employed, such as carbon electrodes, noble electrodes and varieties of dimensionally stable anodes; however, some drawbacks including mass transfer limitation, small space-time yield and low area-volume ratio have intrinsically existed in conventional two-dimensional electrodes[16-17]. The emerging of three-phase three-dimensional electrodes has provided a good solution to the above disadvantages, and the introduction of fragmental materials can provide high specific surface area and enhance the mass transfer for catalytic reactions, bringing about higher removal efficiency[18-20]. However, the obvious free-interconnection and large consumption of granular materials are inevitable and the re-collection is still a problem.

The origination of three-dimensional (3D) porous architectures has given a new sight, and three-dimensional arrangements have been recently able to solve these limitations by establishing 3D porous frameworks as the structural backbone. And ideal 3D architecture electrodes can follow the characterizations: i) it has a porous framework with high interconnection and good electronic conductivity; ii) the

material ensures an improved electrode kinetics and mass transport and provides high accessible surface area; and, iii) the material as a whole is monolithic or self-supported so that no organic binder is needed for electrode fabrication[21-24].

In this work, we used a facile method to fabricate successfully 3D macroporous PbO_2 foam electrode that totally meets above requirements. The easy construction of 3D macroporous network architecture is the key to our fabrication process. The macroporous structure is very helpful to the access of electrolyte to the electrode surface and providing high specific surface area. The structure features of this electrode can be expected to provide superior catalytic performance for efficiently degrading organic contaminants.

Experimental

Carbon nanotube (CNT) sponge substrate was synthesized according to the Reference[25]. A macroporous commercially available sponge was cleaned by ethanol for several times, followed by completely drying and cutting into small pieces with a size of 2mm×10mm×15mm. Tailored sponges were dipped into CNT ink with sodium dodecylbenzene sulfonate as a surfactant, then removed and dried. The dipping-drying process was repeated for several times to increase CNT loading. Finally, the CNT sponges were dried in an oven at 100 °C for 24 h.

The 3D macroporous PbO_2 foam electrode was prepared by the electrodeposition method. The as-prepared CNT sponge and stainless steel plate served as the anode

and cathode, respectively. The composition of electrodposition bath was 150 g L^{-1} $Pb(NO_3)_2$ and 0.5 g L^{-1} NaF, and the pH was adjusted to 0.5~2 through dropping the concentrated nitric acid. The electrodeposition process was conducted at room temperature with a constant current of 40 mA for 2 h. Finally, the 3D PbO_2 foam electrode was washed by distilled water and dried. Titanium-based PbO_2 electrode with the same apparent area was prepared as the control sample in the same condition except the CNT loading process. The fabrication process of 3D PbO_2 foam electrode is schematically illustrated in the following Figure 1.

Electrodes were characterized by scanning electron microscope (SEM, INSPECT S50, MAKE FEI, America) and X-ray diffractometer (XRD, Cu Kα radiation, 40 kV and 150 mA; X'Pert PRO, Netherlands).

The electrochemical dye decolorization experiments were performed in 50 mL 500 mg L^{-1} dye solution with the supporting electrolyte of 0.25 M Na_2SO_4 solution. The operating condition was the room temperature and the galvanostatic condition of 80 mA with a stainless steel plate as the counter electrode. The decolorization processes of dyes were monitored by a UV-vis absorbance spectroscope (Agilent UV-Vis 8453, America), and dye solution concentrations were measured by the absorbance intensity at the characteristic wavelengths of 552 nm for rhodamine B, 664 nm for methylene blue, and 484 nm for orange II.

Results and discussion

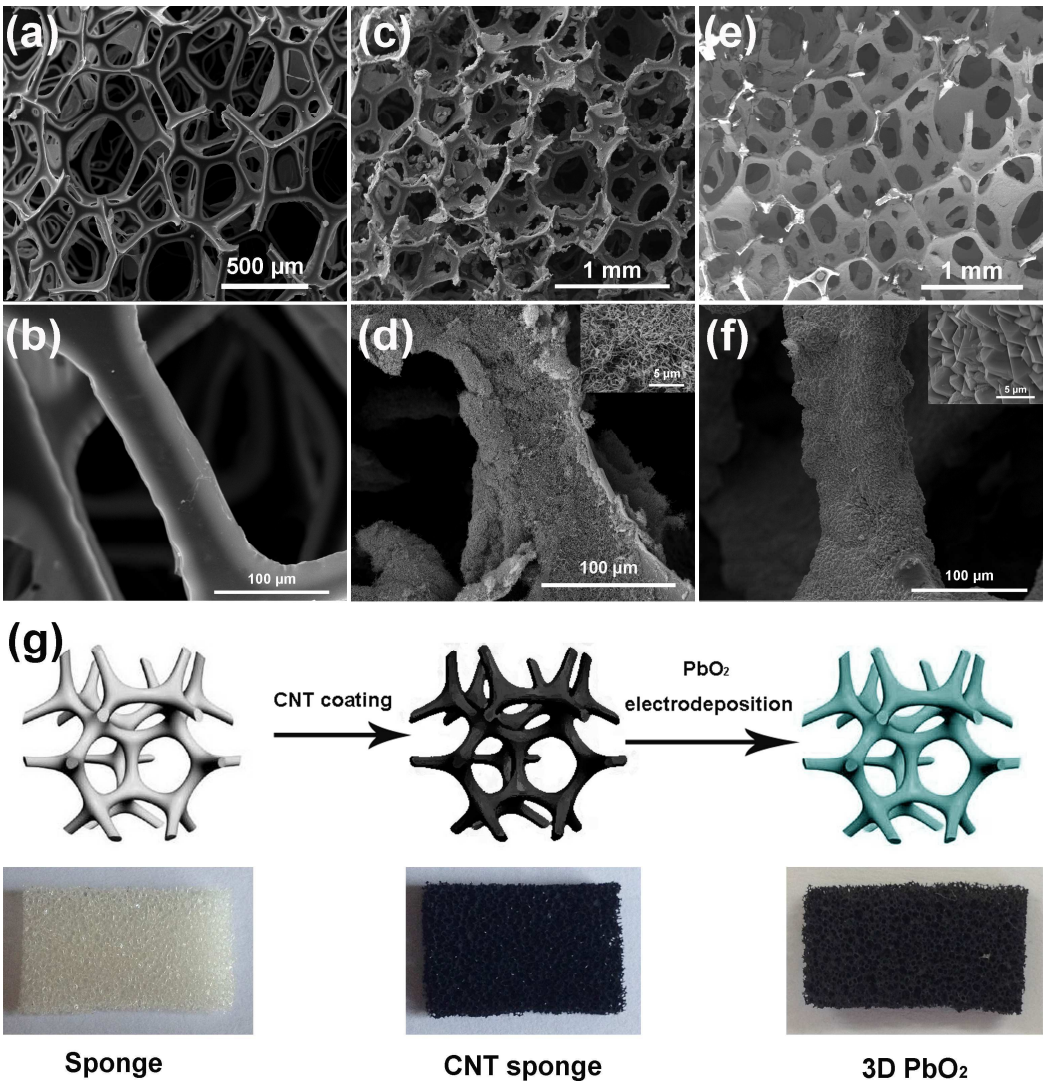

Figure 1 SEM images of (a) and (b) bare sponge, (c) and (d) CNT sponge, and (e) and (f) 3D PbO_2 foam electrode; (g) the schematic illustration of the fabrication process of 3D PbO_2 foam electrode. The insets are the corresponding high magnifications.

Sponge with appropriate aperture was employed as the matrix skeleton network for PbO_2 anode. The network structure of sponge provides with continuously through macropores and high specific surface area: connectivity of macropores can provide

the convenience for liquid flowing, thus benefits the fast mass transport; high specific surface area can increase the loading capacity per unit area and is helpful to enhancing the catalytic ability of catalysts. Comparing with other kinds of 3D framework, sponge is smoothly constructed by three-dimensional polyester fibers and has no knots; this distinct 3D architecture is advantageous to acting as the continuous supporter for catalyst materials and guarantees the continuity and connectivity for the prepared three-dimensional materials. Additionally, sponge has the feature of low costs. Hence, sponge matrix is one of ideal templates to construct three-dimensional materials. The SEM image of sponge is shown in Figure 1a and displays a uniform and smooth network. After immersion-coating carbon nanotube, the branch of sponge displays a rough surface. The flexibility of carbon nanotube and the strong adhesion of the sponge provide an ease to wrapping carbon nanotube around the sponge framework, just as the skin wraps tightly onto the fiber surface. And after electrochemically loading PbO_2, sponge is completely covered with PbO_2 and displays a compact grain layer. Different from planar PbO_2 electrode (Figure S1 shows its SEM image), 3D PbO_2 foam displays refined compact grains with no cracks. This result can be due to the effects of sponge substrate and carbon nanotube. Furthermore, 3D PbO_2 foam possesses highly-through three-dimensional channel framework and large specific surface area: highly-through 3D structure can provide a convenience for fast mass transport; large specific surface area can provide lots of contacts catalytic active sites for contaminant removal and hence enhances the catalytic activity of electrode.

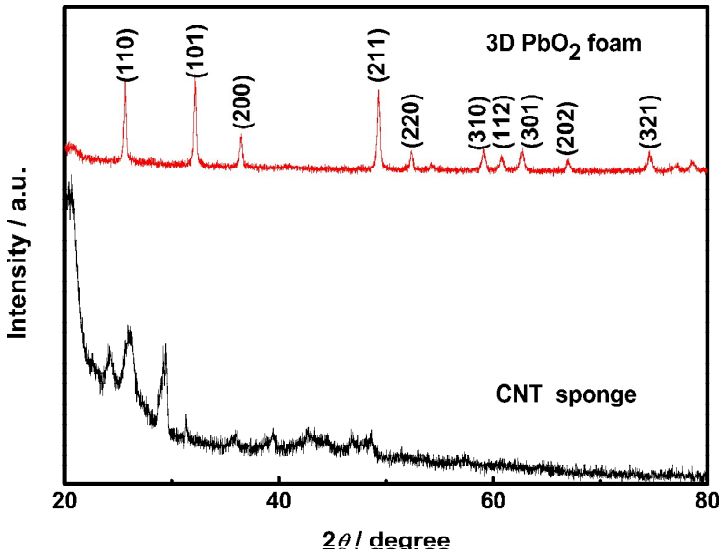

Figure 2 XRD patterns of CNT sponge and 3D macroporous PbO_2 foam electrode.

Figure 2 shows the XRD patterns of CNT sponge and 3D PbO_2 foam electrode. The diffraction peak positions for PbO_2 electrode coincide with those of tetragonal PbO_2 (PDF#41-1492) with the diffraction peaks at (110), (101), (200), (211), (220), (310), (112), and (301), clearly showing the characteristic reflection of β-PbO_2. The three strongest peaks are at (110), (101) and (211) planes, respectively, suggesting the preferred orientation along the (110), (101) and (211) crystallographic directions. The XRD pattern of plate PbO_2 electrode is shown in Figure S1 and has three strongest diffraction peaks at (110), (211) and (301) planes, respectively, which is different from that of 3D PbO_2 foam. This result can be ascribed to the induced effect of carbon nanotube templates. Furthermore, the cell parameters of both electrodes were evaluated according to Bragg's formula. The results are a=b=4.956 Å and c=3.388 Å for standard PbO_2, a=b=5.697 Å and c=4.030 Å for plate PbO_2 electrode, and

a=*b*=4.909 Å and *c*=3.373 Å for 3D PbO_2 foam. This result shows that 3D PbO_2 foam possesses decreased cell parameters. Some literatures suggested that nano-carbon materials such as grapheme and CNT have an inductive effect on the growth or deposition of metal oxides, increases the forming of crystal nucleus and inhibits the grain growth[13-14, 26-27]. Thus the introduction of CNT can benefit the crystal grain refinement, and the result confirms this. Furthermore, the result shows that 3D PbO_2 possesses decreased cell parameters. It is considered that the lattice contraction induces the lattice defects, and these defects can provide active sites and enhance the catalytic activity.

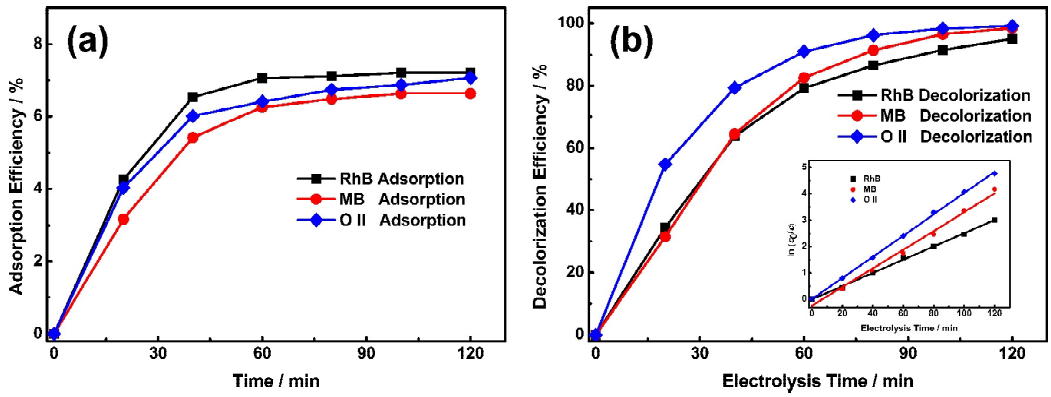

Figure 3 Variations of (a) adsorption efficiency, and (b) decolorization efficiency with time.

To investigate the electrocatalytic ability of 3D PbO_2 foam electrode, two kinds of dyes, azo free dyes (rhodamine B and methylene blue) and azo dye (orange II), were selected as the target contaminants. Firstly, dye adsorption experiments were performed on 3D PbO_2 foam to exclude the effect of carbon nanotube on dye adsorption. Figure 3a shows the variation of dye adsorption with time, the adsorption

equilibriums are reached just within 40 min and the efficiencies are only around 9%. This result indicates that the carbon nanotube sponge is closely covered with amounts of lead oxides and that a good adhesion between sponge substrate and active oxide layer is realized. Electrochemical dye (rhodamine B, methylene blue and orange II) decolorization processes were performed in a galvanostatic condition of 20 mA cm^{-2} with the initial dye concentration of 500 mg L^{-1} and the supporting electrolyte of 0.25 M Na_2SO_4, and the results are shown in Figure 3b. High concentrations of dyes are decolored efficiently on 3D PbO_2 foam, exhibiting the high catalytic activity of 3D PbO_2 foam. The inset of Figure 3b shows the semi-log relationship of dye concentration with electrolysis time, demonstrating that the catalytic decolorization processes follow the first-order kinetics model. The decolorization processes on plate PbO_2 electrode are shown in Figure S4. Compared with plate PbO_2 electrode, the 3D PbO_2 foam exhibits a much higher catalytic efficiency. Figure 4 shows the stability test results of 3D PbO_2. The cyclic stability results show that the decolorization efficiency of 3D PbO_2 electrode still reaches 99 % after use for five times, and confirm a high efficiency for the electrocatalyitc dye decolorization. Meanwhile, the cell potential is stable during the decolorization process; this result shows a good long-term stability. Figure 4b shows the SEM image of 3D PbO_2 electrode after stability test, and most of the parts exhibit a good coverage with the active PbO_2 layer.

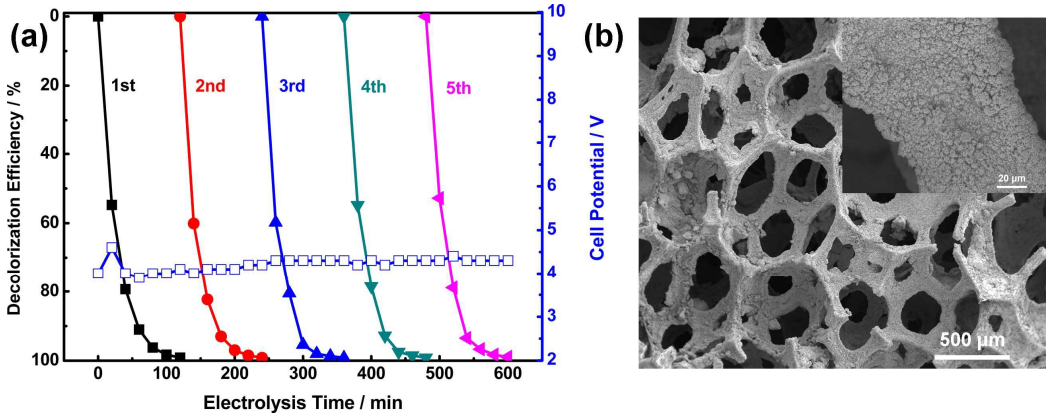

Figure 4 (a) Stability test of 3D PbO_2; (b) SEM image of 3D PbO_2 after stability test.

Some reaction parameters between planar PbO_2 and 3D PbO_2 foam were calculated (their calculation procedures are shown in the Supporting Information) and a comparison is shown in Table 1. The electrochemical impedance results suggest a significantly improved electrochemical activity for 3D PbO_2, and this improved activity can be ascribed to both the construction of 3D sponge-like structure and the effect of CNTs. And the calculated results of diffusion coefficients also confirm the faster mass transfer on 3D PbO_2. All these results demonstrate the excellent advantages of 3D PbO_2 foam.

Table 1 Reaction Parameters on planar PbO_2 and 3D PbO_2 foam.

		Planar PbO_2	3D PbO_2 foam
Electrochemical impedance / ohm		410	29.2
Diffusion coefficient / $cm^2\ s^{-1}$		2.29×10^{-6}	41.8×10^{-6}
First-order kinetics	RhB	6.91×10^{-3}	25.2×10^{-3}
constants for dye	MB	9.39×10^{-3}	35.5×10^{-3}
decolorization / min^{-1}	O II	10.0×10^{-3}	40.2×10^{-3}

Conclusions

In summary, we have developed the three-dimensional macroporous framework to facilely construct the novel structured PbO_2 electrode. This PbO_2 electrode exhibits the structure of three-dimensional uniform foam and high catalytic efficiency for dye treatment in wastewater. Furthermore, we expect that the three-dimensional PbO_2 foam approach described in our work may provide new opportunities to develop the three-dimensional electrocatalytic electrode.

Acknowledgements

The project was supported by the National Natural Science Foundation of China (No. 21476053 and No. 51179033), the Doctoral Program of the Ministry of Education (No. 20132304110027), the Fundamental Research Funds for the Central Universities (No.

HEUCF201403019), and the Fundamental Research Operating Expense for the Central Universities (No. HEUCFD1417).

References

[1] M. Pera-Titus, V. García-Molina, M. A. Baños, J. Giménez, S. Esplugas, *Appl. Catal. B-Environ.*, 2004, **47**, 219.

[2] S. Stolte, S. Abdulkarim, J. Arning, A.-K. Blomeyer-Nienstedt, U. Bottin-Weber, M. Matzke, J. Ranke, B. Jastorff, J. Thoeming, *Green Chem.*, 2008, **10**, 214.

[3] C. A. Martínez-Huitle, E. Brillas, *Appl. Catal. B-Environ.*, 2009, **87**, 105.

[4] C. A. Martínez-Huitle, S. Ferro, *Chem. Soc. Rev.*, 2006, **35**, 1324.

[5] M. Panizza, G. Cerisola, *Chem. Rev.*, 2009, **109**, 6541.

[6] I. Oller, S. Malato, J. A. Sánchez-Pérez, *Sci. Total Environ.*, 2011, **409**, 4141.

[7] C. Feng, N. Sugiura, S. Shimada, T. Maekawa, *J. Hazard. Mater.*, 2003, **B103**, 65.

[8] Á. Anglada, A. Urtiaga, I. Ortiz, *J. Chem. Technol. Biotechnol.*, 2009, **84**, 1747.

[9] B. P. Chaplin, *Environ. Sci.: Processes Impacts*, 2014, **16**, 1182.

[10] G. H. Chen, *Sep. Purif. Technol.*, 2004, **38**, 11.

[11] X. Yang, R. Zou, F. Huo, D. Cai, D. Xiao, *J. Hazard. Mater.*, 2009, **164**, 367.

[12] Y. Liu, H. Liu, J. Ma, J. Li, *Electrochim. Acta*, 2011, **56**, 1352.

[13] X. Duan, F. Ma, Z. Yuan, L. Chang, X. Jin, *Electrochim. Acta*, 2012, **76**, 333.

[14] X. Duan, F. Ma, Z. Yuan, L. Chang, X. Jin, *J. Electroanal. Chem.*, 2012, **677-680**, 90.

[15] S. Ghasemi, H. Karami, H. Khanezar, *J. Mater. Sci.*, 2014, **49**, 1014.

[16] S. Trasatti, *Electrochim. Acta*, 2000, **45**, 2377.

[17] C. Zhang, Y. Jiang, Y. Li, Z. Hu, L. Zhou, M. Zhou, *Chem. Eng. J.*, 2013, **228**, 455.

[18] X. Wu, X. Yang, D. Wu, R. Fu, *Chem. Eng. J.*, 2008, **138**, 47.

[19] L. Yan, H. Ma, B. Wang, Y. Wang, Y. Chen, *Desalination*, 2011, **276**, 397.

[20] W. Liu, Z. Ai, L. Zhang, *J. Hazard. Mater.*, 2012, **243**, 257.

[21] S. Nardecchia, D. Carriazo, M. L. Ferrer, M. C. Gutiérrez, F. del Monte, *Chem. Soc. Rev.*, 2013, **42**, 794.

[22] S. Chabi, C. Peng, D. Hu, Y. Zhu, *Adv. Mater.*, 2014, **26**, 2440.

[23] V. Chabot, D. Higgins, A. Yu, X. Xiao, Z. Chen, J. Zhang, *Energy Environ. Sci.*, 2014, **7**, 1564.

[24] B. Chen, Q. Ma, C. Tan, T.-T. Lim, L. Huang, H. Zhang, *Small*, 2015, **11**, 3319.

[25] X. Xie, M. Ye, L. Hu, N. Liu, J. R. McDonough, W. Chen, H. N. Alshareef, C. S. Criddle, Y. Cui, *Energy Environ. Sci.*, 2012, **5**, 5265.

[26] J. Liu, Z. Guo, F. Meng, Y. Jia, J. Liu, *J. Phys. Chem. C*, 2008, **112**, 6119.

[27] L. Zhang, L. Xua, J. He, J. Zhang, *Electrochim. Acta*, 2014, **117**, 192.